

Effect of multi-cycle heat treatment and pre-history dependence on partial thermoremanence (pTRM) and pTRM tails

Yongjae Yu^{*}, Lisa Tauxe

Geosciences Research Division, Scripps Institution of Oceanography, La Jolla, CA 92093-0220, USA

Received 13 December 2005; received in revised form 7 April 2006; accepted 13 April 2006

Abstract

We test two fundamental assumptions embedded in Thellier experiments, the initial state dependence and the effect of multi-cycle heat treatment. We observe that the magnitude of partial thermoremanent magnetizations (pTRMs) imparted on an initial state of thermal demagnetization is larger than those of pTRMs in the presence of a TRM when the field used to impart pTRM is equal in magnitude and parallel to that used to produce TRM. A multi-cycle Thellier analysis on coarse-grained magnetites progressively produces more intense pTRMs and progressively erases more of the pTRM tails. Both pre-history and multi-cycle dependence will likely enhance the non-linear features of the Arai plot for coarse-grained magnetites.

© 2006 Elsevier B.V. All rights reserved.

Keywords: Paleointensity; Magnetite; Thermoremanent magnetization (TRM); Partial TRM (pTRM); pTRM tail

1. Introduction

There are a number of laboratory protocols for determining absolute paleomagnetic field intensity from archeological and geological materials. Among the various techniques, the Thellier-type paleomagnetic field intensity determination (Thellier and Thellier, 1959) is considered to be most reliable because it can test the fundamental principles of additivity, independence, and reciprocity of partial thermoremanent magnetizations (pTRMs) in the experimental design. In the Thellier-type double heating experiments, we replace the natural remanent magnetization (NRM) produced by an original magnetic field (H_1) with successive pTRMs produced in a laboratory field (H_2) by repeated heating and cooling in the presence of H_2 .

Depending on the sequence of laboratory heating steps three commonly used protocols have been defined. The classical Thellier technique (Thellier and Thellier, 1959) combines two in-field step heatings ($+H_2$ and $-H_2$). At each temperature, the vector sum and vector subtraction provide NRM lost and pTRM gained, respectively. In the most commonly used method of Coe (1967), we first carry out a zero-field heating to determine the NRM lost directly. The pTRM gained is determined from a subsequent in-field heating. The Aitken method (Aitken et al., 1988) takes an opposite approach, by imparting the pTRM before carrying out zero-field heating.

On the basis of a simple mathematical model, recent studies (Yu et al., 2004; Yu and Tauxe, 2005) found that the three techniques for paleointensity are functionally different from one another. Somewhat surprisingly, each method yields quite a different outcome as the reciprocity constraint requiring identical blocking and unblocking temperatures is progressively violated (e.g.,

^{*} Corresponding author.

E-mail address: yju@ucsd.edu (Y. Yu).

Biggin and Bohnel, 2003; Yu et al., 2004). This non-intuitive outcome results from the angular dependence of high unblocking pTRM tails (the portion of a pTRM acquired at a given temperature which is not demagnetized at the same temperature). By far the most efficient method, for identifying the failure of reciprocity, is the IZZI method (Tauxe and Staudigel, 2004; Yu et al., 2004), which alternates the Aitken (in-field and zero-field sequence) and the Coe (zero-field and in-field sequence) methods. The IZZI method can easily detect the angular dependence of pTRM tails, hence the failure of the reciprocity requirement in the Thellier-type experiment.

In the simplest case, there are two different types of pTRMs (Vinogradov and Markov, 1989). We will denote them as $\text{pTRM}\downarrow(T_i, T_0)$ and $\text{pTRM}\uparrow(T_i, T_0)$ (see Table 1). To produce a $\text{pTRM}\downarrow(T_i, T_0)$, we heat a sample in zero field to the Curie point (T_c) and cool it in zero field to the upper end of the blocking temperature

Table 1
Definitions of pTRM and pTRM tails

Abbreviations	Experimental sequence
$\text{pTRM}\downarrow(T_i, T_0)$	(1) Heating from T_0 to the Curie point (T_c) in zero field (2) Cooling from T_c to T_i in zero field (3) Cooling from T_i to T_0 in a lab field \mathbf{H}
$\text{pTRM}\uparrow(T_i, T_0)$	(1) Heating from T_0 to T_i in zero field (2) Cooling from T_i to T_0 in a lab field \mathbf{H}
$t\downarrow(T_{ub} > T_i)$	(1) Producing $\text{pTRM}\downarrow(T_i, T_0)$ (2) Reheating from T_0 to T_i in zero field (3) Cooling from T_i to T_0 in zero field
$t\uparrow(T_{ub} > T_i)$	(1) Producing $\text{pTRM}\uparrow(T_i, T_0)$ (2) Reheating from T_0 to T_i in zero field (3) Cooling from T_i to T_0 in zero field
$\text{pTRM}\uparrow^0(T_i, T_0)$	(1) Thermal demagnetization (cooling from 600 °C in zero-field) (2) Producing $\text{pTRM}\uparrow(T_i, T_0)$
$t\uparrow^0(T_i, T_0)$	(1) Producing $\text{pTRM}\uparrow^0(T_i, T_0)$ (2) Reheating from T_0 to T_i in zero field (3) Cooling from T_i to T_0 in zero field
$\text{pTRM}\uparrow^{\text{TRM}}(T_i, T_0)$	(1) Producing TRM (cooling from 600 °C in a field) (2) Heating-Cooling from T_0 to T_i in zero field (NRM lost) (3) Reheating from T_0 to T_i in zero field + Cooling from T_i to T_0 in \mathbf{H} (pTRM gained)
$t\uparrow^{\text{TRM}}(T_i, T_0)$	(1) Producing $\text{pTRM}\uparrow^{\text{TRM}}(T_i, T_0)$ (2) Reheating-Cooling from T_0 to T_i in zero field

spectrum (T_i) at which point the field is turned on and the specimen cooled to room temperature (T_0). To produce a $\text{pTRM}\uparrow(T_i, T_0)$, we heat the specimen in zero-field only to T_i (not to T_c) and cool it in a lab field to T_0 . In both cases, the portions that survive reheating above T_i (the so-called high unblocking tails) are the pTRM tail $t\downarrow$ and $t\uparrow$, respectively (Table 1). The pTRM tail appears when part of a pTRM demagnetizes outside its blocking interval. Both high unblocking tails have unblocking temperatures (T_{ub}) between T_i and T_c , so are denoted as $t\downarrow(T_{ub} > T_i)$ and $t\uparrow(T_{ub} > T_i)$, to differentiate them from the low unblocking tails whose T_{ub} are less than T_i (Table 1).

In a classical rock magnetic investigation, $t\downarrow(T_{ub} > T_i)$ first drew attention because of its key role in (in)validating the additivity law and because of its substantial size for coarse-grained magnetites (e.g., Bol'shakov and Shcherbakova, 1979; Worm et al., 1988). However, it has also been demonstrated that $\text{pTRM}\uparrow$ can have a substantial tail (e.g., Vinogradov and Markov, 1989; Shcherbakov and Shcherbakova, 2001; Carlut and Kent, 2002; Calvallo et al., 2003; Yu and Dunlop, 2003; Yu et al., 2004). Furthermore, $t\uparrow(T_{ub} > T_i)$ has a direct relevance in Thellier experiments (e.g., Shcherbakov and Shcherbakova, 2001; Yu et al., 2004) because this is the type of tail that can be acquired in the in-field step. In fact, $t\downarrow(T_{ub} > T_i)$ is invisible during Thellier experiments where samples have not been reheated to the Curie point except at the last heating step (e.g., Yu and Dunlop, 2003; Yu et al., 2004).

In order to check whether the pTRM acquired in the in-field step is completely removed by zero-field reheating, it is now fashionable to insert a second zero-field step after the in-field step in a modified Coe method (e.g., Riisager et al., 2000; Riisager and Riisager, 2001). This “pTRM tail check” was initially designed to isolate $t\uparrow$. However, the pTRM tail check step actually measures the vectorial difference between $t\uparrow$ (acquired in the in-field step) and $t\downarrow$ (acquired during the original cooling) (Shcherbakov et al., 2001; Yu and Dunlop, 2003). Thus, the pTRM tail check is particularly useful when vectorial information (including the intensity ratio and angular relation between \mathbf{H}_1 and \mathbf{H}_2) is known (see Yu and Tauxe, 2005).

There are two critical assumptions that are embedded in all Thellier-type analyses. The pTRMs and corresponding pTRM tails are assumed to be reproducible over multiple heating steps and to be independent of prior thermal history. These assumptions must be verified. In the present study, we will test the reproducibility and stability of pTRMs and pTRM tails.

Table 2
Sample summary

Sample set	Sample	<i>n</i>	Ref.	T_{UB} (°C)	M_r/M_s	B_c (mT)	B_{cr} (mT)
Single domain (SD)	Tudor Gabbro	8	[1]	580	0.37–0.44	35.2–41.5	58.2–65.2
Pseudo-single-domain (PSD)	An-ei Basalt	4	[2]	580	0.22–0.25	13.8–18.3	34.7–37.1
Multidomain (MD)	Tudor Gabbro	4	[1]	580	0.06–0.09	4.7–8.3	27.4–41.4

n: number of samples used in pTRM experiments; [1] Yu and Dunlop, 2002; [2] Yu, 1998.

2. Samples

In order to test the reproducibility and stability of pTRM and pTRM tails, we used well-defined magnetite-carrying natural samples (Table 2). Because detailed rock magnetic information was published elsewhere, we include here only a short summary of previous work and describe in more detail additional supplementary rock magnetic tests. For a sample set here called SD, with remanence carrying minerals in the single-domain (SD) grain size range, we used eight specimens from the Tudor Gabbro (Ontario, Canada). These yielded apparently excellent paleointensity data in previous studies (Yu and Dunlop, 2001). In particular, these samples have a very narrow unblocking temperature spectrum (most of the remanence was unblocked between 500 and 580 °C). For typical pseudo-single-domain (PSD) and multidomain (MD) sample sets, we used four basalts (Yu, 1998) and four gabbros (Yu and Dunlop, 2002), respectively. These samples in the PSD and MD sets were rejected in previous paleointensity work because of their non-linear Arai plots. Importantly, during the initial paleointensity work, none of the samples from the SD, PSD, or MD sets showed any indication of alteration during repeated heatings; all the samples passed the pTRM check within 5% at all temperature ranges.

For each specimen, room temperature hysteresis was measured on 3–6 chips obtained from a sister specimen. Hysteresis loops were measured in a peak field of 1 T in field increments of 10 mT by using the alternating gradient force magnetometer (AGFM) in the Scripps paleomagnetic laboratory (see example in Fig. 1). Values of saturation magnetization (M_s), saturation remanence (M_r), and coercivity (B_c) were determined from hysteresis loops after nonferrimagnetic slope correction. In addition, values of coercivity of remanence (B_{cr}) were obtained from back-field measurements. In a squareness-coercivity plot (Néel, 1955) where squareness is the ratio M_r/M_s and a Day diagram (Day et al., 1977), each set of samples forms a distinct cluster with average squareness values of ~ 0.40 , ~ 0.22 , and 0.08, respectively (Fig. 1a and b).

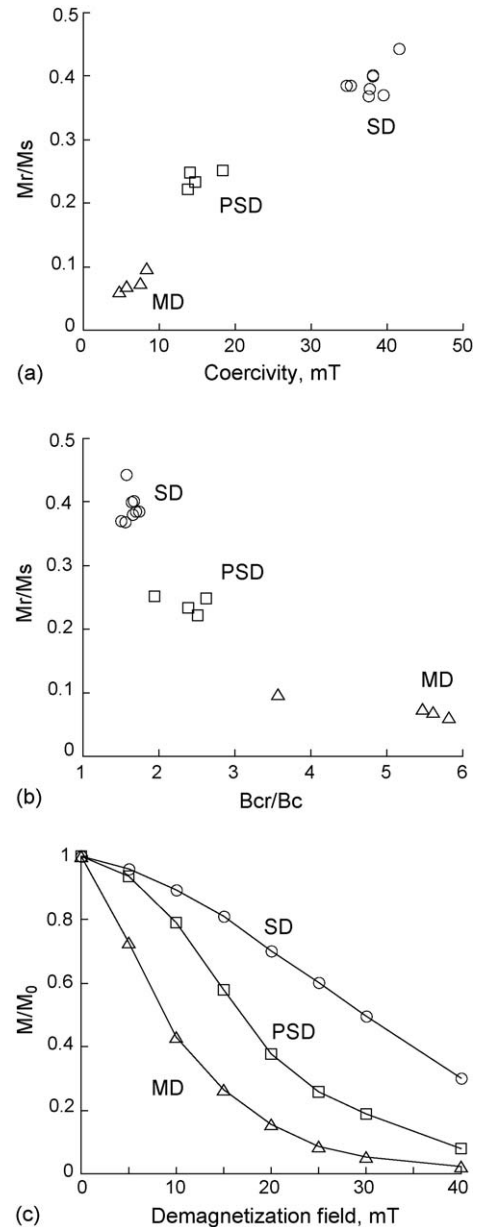


Fig. 1. Hysteresis results in (a) squareness-coercivity plot, and (b) Day diagram. Each sample set forms a distinct cluster in the so-called SD, PSD, and MD regions. Typical hysteresis loops are shown in the insets. (c) As the grain size increases, we observed a rapid demagnetization of ARM at low coercivity.

Representative examples of alternating-field (AF) coercivity spectra of anhysteretic remanent magnetization (ARM) are shown in Fig. 1c. We produced ARM along the cylindrical axis of the specimen in an AF decaying from 120 mT with a superimposed a steady field of $50 \mu\text{T}$. Stepwise AF demagnetization was then carried out. The amount of an initial plateau, a hallmark for the existence of fine-grained magnetite, steadily decreases as the average grain size increases (Fig. 1c).

3. Pre-history dependence

In Thellier-type experiments, we assume that the pTRM produced from a thermally demagnetized state [$\text{pTRM}\uparrow^0(T_i, T_0)$] (as in the original TRM) is equivalent to that produced in samples that have a TRM [$\text{pTRM}\uparrow^{\text{TRM}}(T_i, T_0)$] (as in the laboratory pTRM). This is, in fact, true in the original Thellier method because there is no zero-field cooling step in which to determine the pTRM tail. Mathematical modeling (e.g., Yu et al., 2004) and the phenomenological model of Fabian (2000) also assume the equivalency of the two types of pTRMs. Although the initial state dependence of pTRM intensity has been well recognized (e.g., Vinogradov and Markov, 1989; Shcherbakov and Shcherbakova, 2001; Shcherbakov et al., 2001), a direct comparison of $\text{pTRM}\uparrow^0(T_i, T_0)$ and $\text{pTRM}\uparrow^{\text{TRM}}(T_i, T_0)$ and their practical impact requires further testing.

In order to investigate the relationship of $\text{pTRM}\uparrow^0(T_i, T_0)$ and $\text{pTRM}\uparrow^{\text{TRM}}(T_i, T_0)$, we first produced a $\text{pTRM}\uparrow^0(T_i, T_0)$ from a thermally demagnetized initial state by cooling from 600°C in zero-field to T_0 , then reheating in zero field to T_i , followed by cooling from T_i to T_0 , this time in a lab field. The pTRM tail $t\uparrow^0(T_{\text{ub}} > T_i)$ was measured after reheating to T_i and cooling in zero-field.

To measure $t\uparrow^{\text{TRM}}(T_{\text{ub}} > T_i)$, we performed a pTRM tail check following the procedure of Riisager and Riisager (2001). As an initial state, a TRM was produced by cooling from 600°C to T_0 in a field. Following the first (zero-field) and second (in-field) cooling from T_i to T_0 , samples were heated a third time to T_i and cooled in zero field. This third heating-cooling yields a $\text{pTRM}\uparrow^{\text{TRM}}(T_i, T_0)$. The difference between the remanences measured after the first and third steps is the $t\uparrow^{\text{TRM}}(T_{\text{ub}} > T_i)$. After the third heating, a fourth in-field step to a lower temperature T_{i-1} was carried out to obtain a conventional pTRM check to verify the lack of chemical alteration.

All the remanence measurements in the present study were carried out on a 2G Enterprises three-axis through-bore cryogenic magnetometer. A TRM was produced by cooling from 600°C in a laboratory field of $\mathbf{H}_1 = 50 \mu\text{T}$.

At each heating step, samples were held for 30 min. Measurements were carried out in a magnetically shielded space with an ambient field less than 250 nT. The residual field in the furnace during nominally zero-field heatings was less than 5 nT. Throughout all heating, temperatures were reproducible within 1°C .

Arai plots for four representative samples are given in Fig. 2. Results in Fig. 2 are rearranged in Fig. 3 to represent the temperature dependence of pTRM ($=[\text{pTRM}/\text{TRM}]$) and pTRM tails ($=[\text{pTRM tail}/\text{TRM}]$). The $[\text{pTRM}/\text{TRM}]$ ratio increased as the temperature increased, but most pTRMs are produced when $T_i > 500^\circ\text{C}$ for SD1, SD2, and PSD1 (Fig. 3a and c). The pTRMs were more distributed for the MD samples. PSD1 shows somewhat mixed behavior (Fig. 3c). In addition, as expected, SD1 and SD2 follow perfectly linear Arai plots while PSD shows minor non-linearity and MD reveals a substantial curvature in the Arai plots (Fig. 2). Nevertheless, as shown in other studies (e.g., Yu and Dunlop, 2003; Yu et al., 2004; Yu and Tauxe, 2005), the pTRM tail check is uniformly zero because \mathbf{H}_2 is parallel and of equal magnitude to \mathbf{H}_1 (open squares along the pTRM acquisition axis in Fig. 2; solid symbols in Fig. 3b and d).

The most important observation from the data shown in Figs. 2 and 3 is that $\text{pTRM}\uparrow^0(T_i, T_0)$ is always stronger than $\text{pTRM}\uparrow^{\text{TRM}}(T_i, T_0)$ (Fig. 3a and c). For all the tested samples, $\text{pTRM}\uparrow^0$ was larger than $\text{pTRM}\uparrow^{\text{TRM}}$ for the entire temperature range (Fig. 3a,c). A difference of pTRM intensity between $\text{pTRM}\uparrow^0(T_i, T_0)$ and $\text{pTRM}\uparrow^{\text{TRM}}(T_i, T_0)$ is compared with the pTRM tail ($=t\uparrow^0$) and shows no obvious correlation (Fig. 4). For SD2, $t\uparrow^0(T_{\text{ub}} > T_i)$ and ΔpTRM ($=\text{pTRM}\uparrow^0(T_i, T_0) - \text{pTRM}\uparrow^{\text{TRM}}(T_i, T_0)$) were nearly identical over the entire temperature ranges (Fig. 4). In contrast, $t\uparrow^0(T_{\text{ub}} > T_i)$ was progressively larger than ΔpTRM at $>350^\circ\text{C}$ for MD1 and PSD1 (Fig. 4). In these samples (MD1 and PSD1), the ΔpTRM at $>350^\circ\text{C}$ was nearly constant while $t\uparrow^0$ increased as the temperature increased (Fig. 4). While similar to SD2, SD1 shows slight tendency of $t\uparrow^0 > \Delta\text{pTRM}$ except for the 450°C step, implying small PSD contribution in this sample (Fig. 4).

We also compared the ratios $[t\uparrow^0/\text{pTRM}\uparrow^0]$ and $[t\uparrow^{\text{TRM}}/\text{pTRM}\uparrow^{\text{TRM}}]$ (Fig. 5), as these were proposed as tests for domain state of magnetite (e.g., Shcherbakova and Shcherbakov, 2000). We anticipated that the ratio $[t\uparrow^0/\text{pTRM}\uparrow^0]$ (open symbols in Fig. 5) would be larger for coarse-grained materials because of their prominent tails. However, the ratio $[t\uparrow^0/\text{pTRM}\uparrow^0]$ only partially reflects the magnitude of the total tail hence is a poor indicator of the quality of Thellier experiments (see detailed

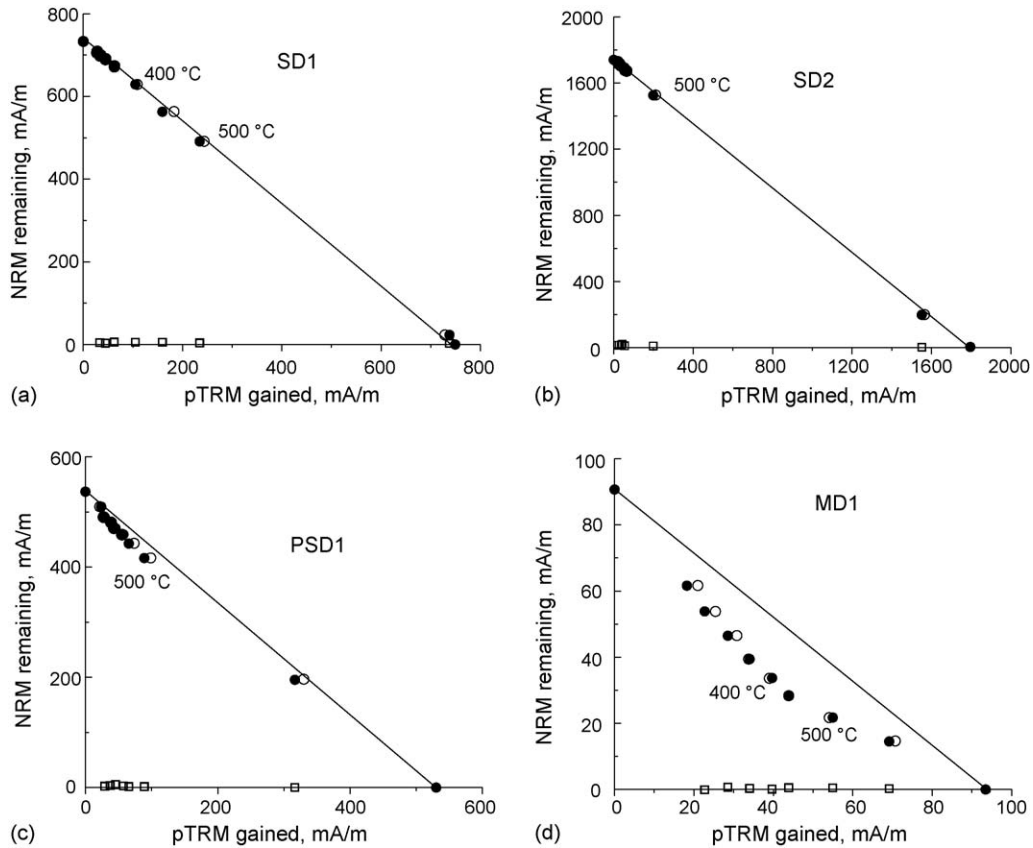


Fig. 2. Examples of Arai plots on a laboratory produced TRM incorporating both pTRM checks and pTRM tail checks. The Arai plots are linear for (a) SD1 and (c) SD2, but are progressively non-linear for (b) MD1 and (d) PSD1. Regardless of the linearity in Arai plots, the pTRM tail checks are uniformly zero because \mathbf{H}_2 was equal and parallel to \mathbf{H}_1 . Solid circles: Thellier experiments; Open circles: pTRM checks; Open squares: pTRM tail checks.

explanation in Section 5). It appears that the usefulness of $[\tau^0/p\text{TRM}^0]$ in paleointensity determinations is limited (Fig. 5 versus Figs. 2, 3b, 3d).

4. Effect of multi-cycle heat treatment

Another fundamental assumption embedded in the Thellier experimental method is that pTRMs and pTRM tails are stable when subjected to multiple heatings. This assumption may not be true, especially for coarse-grained materials, whose magnetizations are continuously driven to more and more stable states during repeated heat treatments, a phenomenon known as “the Markov process” (e.g., Fabian, 2003). Repeated microscopic observations on coarse magnetite show many different configurations of magnetic domains and domain walls (Heider et al., 1988; Heider, 1990; Halgedahl, 1991; Ambatiello et al., 1999). Micromagnetic simulations have also illustrated the existence of multiple local energy minima that are bounded by statistically dis-

tributed energy barriers (Enkin and Dunlop, 1987; Enkin and Williams, 1994; Winkelhofer et al., 1997). In addition, recent studies clearly demonstrated that the multi-cycle demagnetization to T_i , both at high (Biggin and Bohnel, 2003) and at low temperature ranges (Liu and Yu, 2004), progressively erases more remanence. Hence, the magnetization process in coarse grains requires a stochastic approach to fully describe it (e.g., Fabian, 2003).

In the present study, we test whether the remanent magnetization is reproducible under in-field and zero-field conditions, a requirement for successful paleointensity study. Although progressive demagnetization on multiple heating has been observed, the effect of multi-cycle heat treatment on remanence acquisition has not been examined. It is interesting to check the effect of the Markov process under in-field conditions. The second issue is the temperature dependence of the Markov process. It is possible that the amount of progressive demagnetization (or progressive remanence acquisition)

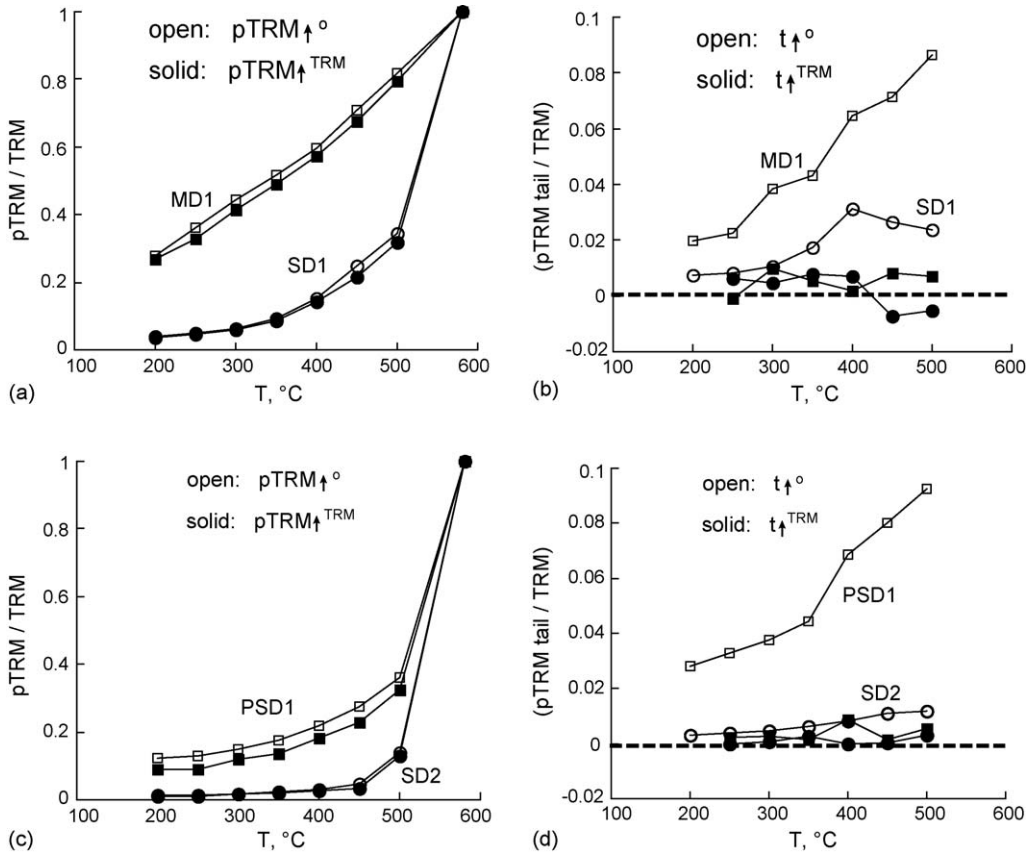


Fig. 3. Variation of $[pTRM/TRM]$ and $[(pTRM \text{ tail})/TRM]$. (a, b) SD1 and MD1, (c, d) SD2 and PSD1. For $[pTRM/TRM]$ ratio, open and solid symbols represent $pTRM\uparrow^\circ$ and $pTRM\uparrow^{TRM}$. For $[(pTRM \text{ tail})/TRM]$ ratio, open and solid symbols represent $t\uparrow^\circ$ and $t\uparrow^{TRM}$, respectively. The effect of pre-history dependence of pTRM is strong for samples with broad blocking temperature spectra (e.g., MD1).

would follow different trends at different temperature intervals (e.g., Liu and Yu, 2004). Overall, we are interested in testing the reproducibility of pTRM acquisition and the pTRM tail check.

We used a total of nine specimens (three selected from each set of SD, PSD, and MD). For three specimens per

set, we produced an initial TRM (in H_1) along z (parallel), $-z$ (anti-parallel), and y (perpendicular) directions, respectively. Then, we carried out a pTRM tail check analysis including three cycles of multiple heatings at the second in-field step and the third pTRM tail check step. We applied H_2 along z in order to check whether

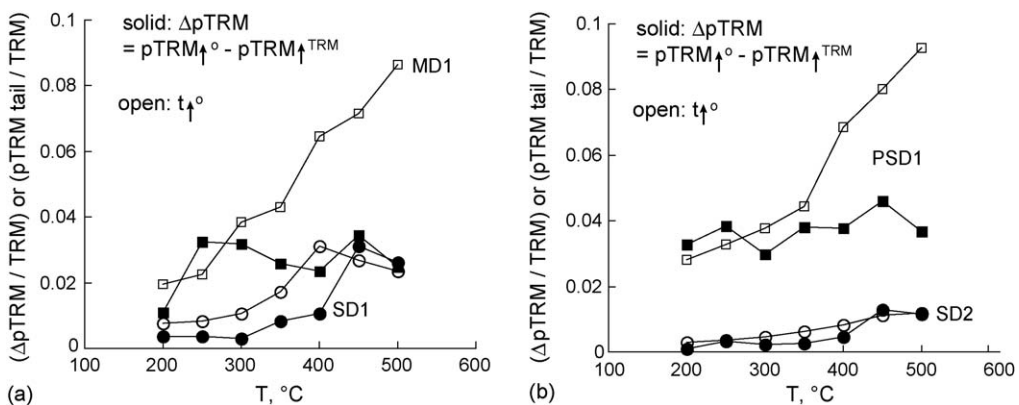


Fig. 4. Comparison of $\Delta pTRM (=pTRM\uparrow^\circ - pTRM\uparrow^{TRM})$ and $t\uparrow^\circ$. The $\Delta pTRM$ and $t\uparrow^\circ$ show no obvious correlation.

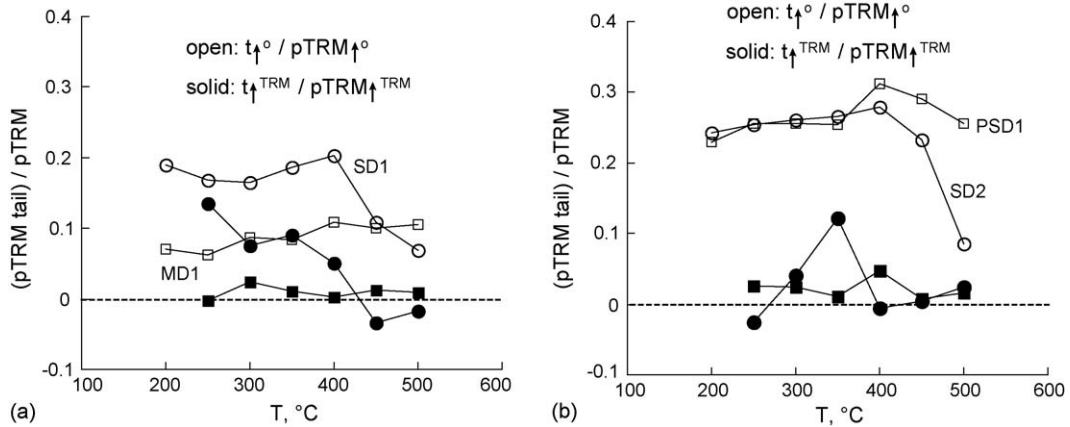


Fig. 5. Comparison of [(pTRM tail)/TRM] for different initial states. The [(pTRM tail)/TRM] is surprisingly large for fine-grained magnetites but small for coarse-grained samples. This apparent irony results from the small values of pTRM at low- to intermediate temperatures, indicating that [(pTRM tail)/TRM] should not be used as a sample selection criterion.

the effect of multi-cycle heat treatments shows an angular dependence (see testing 1 in Table 3).

During the multi-cycle heat treatment, both pTRMs and pTRM tail checks remained relatively constant for the SD samples (Fig. 6a). In contrast, pTRM acquisition progressively increased and pTRM tail checks progressively decreased for MD1 (Fig. 6b). In particular, the pTRM tail checks progressively decreased for the MD sample regardless of the angular configuration (Fig. 6). The results for [pTRM/TRM] and [t^{TRM}] (=pTRM tail check)/TRM] are plotted as a function of temperature (Fig. 7). The progressive increase of [pTRM/TRM] and the progressive decrease of [t^{TRM}] (=pTRM tail check)/TRM] are more prominent as the temperature increases (Fig. 7).

While $p\text{TRM}^{\uparrow}(T_i, T_0)$ and $t^{\text{TRM}}(T_{\text{ub}} > T_i)$ are important because of their direct relevance to Thellier

experiments, $p\text{TRM}^{\uparrow}(T_i, T_0)$ and $t^{\uparrow}(T_{\text{ub}} > T_i)$ are also useful rock magnetic indicators. It is therefore necessary to check the reproducibility of $t^{\uparrow}(T_{\text{ub}} > T_i)$. We first produced a $p\text{TRM}^{\uparrow}(T_i, T_0)$ from a thermally demagnetized initial state by cooling from 600 °C in zero-field to T_0 heating in zero field to T_i , and then cooling from T_i to T_0 in a lab field. The pTRM tail $t^{\uparrow}(T_{\text{ub}} > T_i)$ was measured after reheating to T_i in zero-field. We repeated the last zero-field reheating three times (see testing 2 in Table 3). This entire procedure was performed at seven different temperatures ($T_i = 250, 300, 350, 400, 450, 500,$ and 550 °C). For $T_i = 400$ °C, we repeated the final zero-field reheating 10 times.

We found a progressive decrease of $t^{\uparrow}(T_{\text{ub}} > T_i)$ on repeated heating (Fig. 8a). While the values of $t^{\uparrow}(T_{\text{ub}} > T_i)$ increase as the temperature increases, the rate of change in $t^{\uparrow}(T_{\text{ub}} > T_i)$ is nearly temperature independent (Fig. 8a). As the number of repeated heating increases, the $t^{\uparrow}(T_{\text{ub}} > T_i)$ acquired when $T_i = 400$ °C decreases sub-exponentially (Fig. 8b).

Table 3
Testing the effect of multi-cycle heat treatment

Testing	Experimental sequence
Sequence A	Producing TRM (cooling from 600 °C in a field)
Sequence B	Heating-cooling from T_0 to T_i in zero field
Sequence C	Heating from T_0 to T_i in zero field + cooling from T_i to T_0 in H
Sequence D	Reheating-cooling from T_0 to T_i in zero field
Sequence E	Thermal demagnetization (cooling from 600 °C in zero-field)
Testing 1	(A)-(B)-(C)-(C)-(D)-(D)-(D)
Testing 2	(E)-(C)-(D)-(D)-(D)
Fig. 2 in FS04	(E)-(C)-(D)-(C)-(D)-(C)-(D)
Fig. 5 in FS04	(E)-(C)-(D)-(D)-(D)

We only illustrate three multiple heating sequence for convenience; FS2004: Fabian and Shcherbakov (2004).

5. Discussion

5.1. Pre-history dependence

In the present study, we have experimentally tackled two fundamental assumptions embedded in Thellier experiments. To date, convex-down Arai-plots have been attributed to low unblocking pTRM tails that violate the reciprocity law (e.g., Shcherbakov et al., 2001; Yu and Dunlop, 2003). That is, non-uniformly magnetized particles acquire less magnetization during the in-field step than is destroyed during the zero-field step at a given

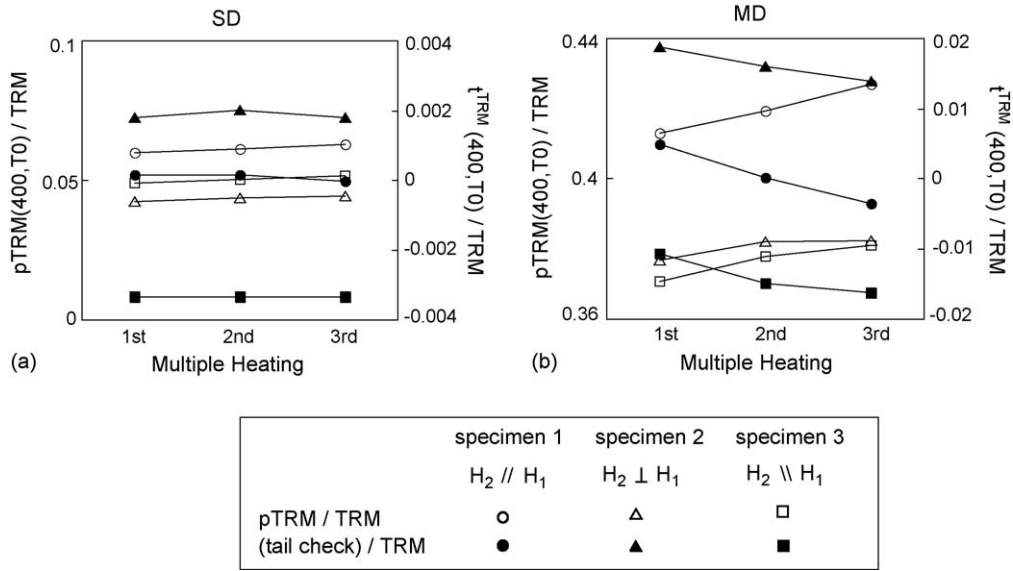


Fig. 6. Variation of intensities of multi-cycle pTRMs and pTRM tail checks. Initial TRM was produced by cooling from 600 °C in H_1 for a total of nine specimens (3 for SD, PSD, and MD, respectively). For each subset of 3 specimens, H_1 was set to z , $-z$, y . We then carried out a pTRM tail analysis. During in-field step, H_2 was applied along the z axis. While values of pTRMs and pTRM tails remain relatively constant for SD, MD samples show a progressive increase in pTRM intensity and a progressive decrease in pTRM tail checks.

temperature. Indeed, this is the major factor that causes the non-linear features in Arai plots (e.g., Yu et al., 2004; Yu and Tauxe, 2005).

Another process that slightly enhances the non-linear features of Arai plots is the pre-history dependence of pTRMs. We found that a pTRM produced from a thermally demagnetized state acquired a more intense remanence than a pTRM generated during the Thellier experiments (Fig. 3). Different initial states are known to affect the thermal demagnetization of pTRM and viscous remanent magnetization of coarse-grained mag-

netites (Vinogradov and Markov, 1989; Halgedahl, 1993; Shcherbakova et al., 2000; Dunlop and Özdemir, 2000, 2001).

We observed a strong initial state dependence for samples with a wide blocking temperature spectrum (e.g., sample MD1 in Fig. 3a). On the other hand, SD1 and SD2 showed little effect (Fig. 3a and c). In summary, a dependence of magnetic properties on prior magnetic history is a hallmark for non-uniformly magnetized materials (Figs. 2–4). It is also notable that the effect of the initial state dependence of pTRM intensity is nearly

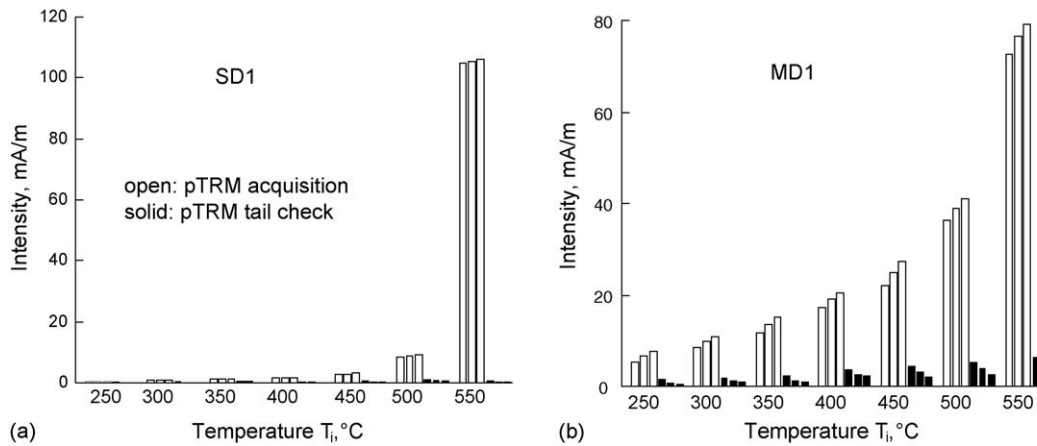


Fig. 7. Variation of intensities of multi-cycle pTRMs and pTRM tail checks as a function of temperature. (a) SD1 shows no obvious impact of multi-cycle heat treatment. (b) For MD1, pTRMs progressively increase while pTRM tail checks progressively decrease.

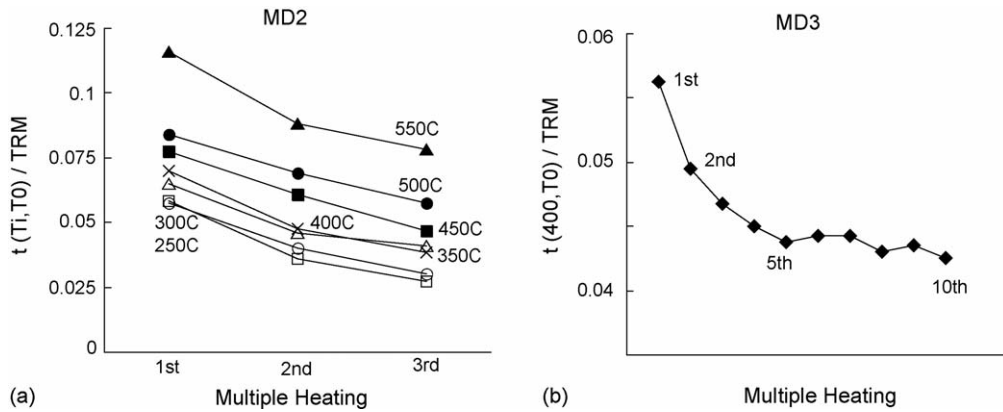


Fig. 8. Effect of multi-cycle heat treatment on pTRM tails ($=t\uparrow$). The pTRM tails progressively decrease as we carry our multiple heatings.

temperature independent (Figs. 3 and 4). In the present study, we only considered the simplest case when the H1 and H2 are equivalent both in magnitude and direction. The drawback of such a condition would be that the pTRM tails are indistinguishable from the remaining TRM fraction because they are parallel to each other. However, equal magnitude and parallel direction between H1 and H2 is used because it is easy to produce and because it is free from the angular dependence.

What causes the initial state dependence of pTRM in MD samples? For the thermally demagnetized initial state, it is plausible that potential walls are more uniformly distributed than those for a corresponding zero-field step in the presence of TRM. In addition, soft domain walls (that will react first in any thermal treatment) for thermally demagnetized states may anchor at deeper potential wells, leading them to be less likely to move under in-field conditions. If so, the remanence acquisition process in the Thellier analysis consumes more energy to escape the energy barriers, leading to a less intense magnetization. Then, a pTRM produced from a thermally demagnetized state acquires more intense remanence than a pTRM generated during the Thellier experiments (Fig. 3). This proposition remains to be shown in the future using microscopic observation or micromagnetic simulation.

What is the link between the initial state dependence of pTRM and the size of the pTRM tail check? This is very important in modeling of Thellier experiments. In simulation of Thellier experiment (e.g., Yu et al., 2004), it is frequently assumed that a pTRM $\uparrow^{\text{TRM}}(T_i, T_0)$ remagnetizes both the reciprocal fraction $r\uparrow^{\text{TRM}}(T_0 < T_{\text{ub}} < T_i)$ (i.e., this is the fraction which is demagnetized at the same temperature where the pTRM was acquired) as well as the high temperature tail $t\uparrow^{\text{TRM}}(T_{\text{ub}} > T_i)$. A few recent phenomenological models (e.g., Biggin and

Bohnel, 2003; Krasa et al., 2003; Leonhardt et al., 2004) also adopt a similar approach by introducing regions for $r\uparrow^{\text{TRM}}$ and $t\uparrow^{\text{TRM}}$, while the initial model (Fabian, 2000, 2001) was only valid for $t\downarrow$. However, the initial state dependence of pTRM shows a weak temperature dependence, and shows no apparent correlation with the magnitude of the pTRM tails (Fig. 4). This lack of correlation is particularly noticeable for the samples with prominent tails (Fig. 4). Furthermore, $t\uparrow^{\text{TRM}}(T_{\text{ub}} > T_i)$ has been observed to be erased by multiple reheatings (Fabian and Shcherbakov, 2004). To this end, it is clear that none of the proposed phenomenological models or mathematical models can explain the observed features (in particular the role of $t\uparrow^{\text{TRM}}$), thus those models require revision. The results in Fig. 4 clearly indicate that the initial state dependence of pTRM is a fundamental property of pTRM and is independent of the pTRM tail.

How much difference does the initial state dependence of pTRM cause in Thellier experiments? According to our experiment, the intensity difference between pTRM \uparrow^0 and pTRM \uparrow^{TRM} is 3–4% for PSD and MD samples that showed convex-down Arai plots (Figs. 3 and 4). For our SD samples, the difference was negligible (Fig. 4). In practice, the initial state dependence of pTRM would amplify the non-linear convex-down features in Arai plots by underestimating the pTRM acquisition by a few % (Fig. 4). However, this aspect is unlikely to change the outcome of paleointensity determinations since reliable samples with minimal tails are almost free from the initial state dependence of pTRM (Figs. 2–4).

It is worthy of note that a difference between pTRM $\uparrow^0(T_i, T_0)$ and pTRM $\uparrow^{\text{TRM}}(T_i, T_0)$ for coarse-grained samples is a maximum estimate of initial state dependence of pTRM. As a matter of fact, pTRM $\uparrow^{\text{TRM}}(T_i, T_0)$ experienced one more heating

step than the $p\text{TRM}\uparrow^0(T_i, T_0)$. Besides the first heating for producing initial TRM, $p\text{TRM}\uparrow^{\text{TRM}}(T_i, T_0)$ requires demagnetization to T_i prior to $p\text{TRM}$ acquisition. To match up the number of heatings, it would be fair to insert another partial demagnetization to T_i between initial thermal demagnetization and later $p\text{TRM}$ acquisition for $p\text{TRM}\uparrow^0(T_i, T_0)$. In fact, Shcherbakov and Shcherbakova (2001) have shown that inserting another demagnetization step prior to the in-field step slightly reduced the $p\text{TRM}$ intensity (we will denote it as $p\text{TRM}\uparrow^{00}(T_i, T_0)$). Thus, $\Delta p\text{TRM}$ is a maximum estimate of the pre-history dependence effect. We produced a $p\text{TRM}\uparrow^0(T_i, T_0)$ without another partial demagnetizing step for practical reason. For example, the absolute capacity in acquiring $p\text{TRM}$ from a demagnetized state is $p\text{TRM}\uparrow^0(T_i, T_0)$, which has been frequently used in rock magnetic study. In addition, a commonly used parameter as a criterion in selecting suitable samples for paleointensity (e.g., tail to $p\text{TRM}$ ratio, Shcherbakov and Shcherbakova, 2000) is $p\text{TRM}\uparrow^0(T_i, T_0)$ not $p\text{TRM}\uparrow^{00}(T_i, T_0)$.

Is the ratio of $[(p\text{TRM tail})/p\text{TRM}]$ useful in the paleointensity determination? The ratio $[t\uparrow^0/p\text{TRM}\uparrow^0]$ has been suggested as a pre-selection criterion (e.g., Shcherbakov and Shcherbakova, 2001). Yet, contrary to expectation, these parameters fail to discriminate acceptable samples from the unacceptable ones. For example, SD1 and SD2 showed surprisingly high $[t\uparrow^0/p\text{TRM}\uparrow^0]$ ratios (Fig. 5), although they showed nearly ideal behavior in the Arai plots (Fig. 3). The irony lies in the fact that the intensities of $p\text{TRMs}$ and $p\text{TRM}$ tails are both very small for less than 500 °C for SD samples (Fig. 5), hence any experimental error or instrumental noise apparently makes their ratio impractical (Fig. 5). In practice, the use of $[t\uparrow^0/p\text{TRM}\uparrow^0]$ ratio should be restricted for samples containing coarse-grained materials or only at high temperature ranges where $p\text{TRM}$ can reasonably represent significant portions of TRM. Universal application of the $[t\uparrow^0/p\text{TRM}\uparrow^0]$ ratio as a selection criterion in Thellier analysis may discard what are otherwise acceptable results (e.g., Fig. 2 versus Fig. 5).

5.2. Effect of multi-cycle heat treatment

Without alteration in mineralogy, the values of $p\text{TRM}$ gained and the $p\text{TRM}$ tail check must remain constant throughout the multi-cycle heat treatments for a successful Thellier analysis. Indeed, both $p\text{TRM}$ acquisition and $p\text{TRM}$ tail checks were nearly unchanged for SD1, validating the expectation (Figs. 6a and 7a). In this sample, the multiple heating caused less than 1% variation of $p\text{TRM}$ acquisition (Fig. 6a). However, MD1 shows

quite different features (Figs. 6b and 7b). The values of the $p\text{TRM}$ gained progressively increased while those of the $p\text{TRM}$ tail check progressively decreased (Fig. 6b). All these observations are independent of the angular relation between \mathbf{H}_1 and \mathbf{H}_2 (Fig. 6). A general trend of increasing $p\text{TRM}$ intensity in multiple repeated heating is in excellent agreement with the observed features in Biggin and Bohnel (2003).

One may wonder why the $p\text{TRM}$ tail check was zero in Fig. 2 but was always positive in Fig. 7, although we applied the same technique on the same set of samples. The answer lies in the angular dependence of $p\text{TRM}$ tails. Note that a $p\text{TRM}$ tail check ($t\uparrow^{\text{TRM}}$) measures the vectorial difference between the high-temperature tails of $p\text{TRM}\uparrow$ and the pre-existing high-temperature tails $p\text{TRM}\downarrow$ that are embedded in TRM (e.g., Shcherbakov et al., 2001; Yu and Dunlop, 2003; Yu et al., 2004; Yu and Tauxe, 2005). As predicted and tested previously (e.g., Yu et al., 2004), $p\text{TRM}$ tail checks are zero, positive, and negative for \mathbf{H}_2 parallel, perpendicular, and anti-parallel to \mathbf{H}_1 with equal magnitude (Fig. 6). In fact, the intensity and sign of the $p\text{TRM}$ tail check depend on the intensity ratio as well as the angular relationship between \mathbf{H}_1 and \mathbf{H}_2 .

For the thermally demagnetized initial state, our observation is in excellent agreement with the trend reported by Fabian and Shcherbakov (2004). In both studies, exponential decay of remanent magnetization for $[t\uparrow^0]$ was observed (testing 2 in Fig. 8b; see also Fig. 4b in Fabian and Shcherbakov (2004)). Domain state stabilization in coarse-grained samples was suggested as a source of decaying behavior on $[t\uparrow^0]$ (Fabian and Shcherbakov, 2004). It is possible that a systematic decrease of $[t\uparrow^{\text{TRM}}]$ (Figs. 6 and 7) shares the same physical origin.

For the initial TRM condition, we measured the stability of $[p\text{TRM}\uparrow^{\text{TRM}}]$ and $[t\uparrow^{\text{TRM}}]$ separately. Examining the stability of $[p\text{TRM}\uparrow^{\text{TRM}}]$ and $[t\uparrow^{\text{TRM}}]$ is necessary because these are the types of remanences that are produced in real Thellier experiments. In MD grains, the progressive variation both for $p\text{TRM}$ acquisition and the $p\text{TRM}$ tail check was the largest in the second heating, then the increment/decrement decreased in the third heating (Fig. 7b). In terms of an absolute scale, the progressive variation of magnetization increased as the temperature increased (Fig. 7). However, in terms of percent increment (normalized to corresponding $p\text{TRM}$), the effect of the progressive increase of $p\text{TRM}$ intensity was larger at low temperatures (up to 20%) than at high temperatures (6–12%). At a given temperature, the amount of progressive changes of magnetization was usually three times bigger for the in-

field (pTRM acquisition) setting than for the zero-field (pTRM tail check) one (Fig. 7b). If we measure the combined stability of $[\text{pTRM}\uparrow^{\text{TRM}}] + [t\uparrow^{\text{TRM}}]$, it is likely that the overall magnitude increases because the cumulative multi-cycle effect of $\text{pTRM}\uparrow^{\text{TRM}}(T_i, T_0)$ outweighs that of $t\uparrow^{\text{TRM}}(T_{\text{ub}} > T_i)$ (Figs. 6 and 7). In fact, Fabian and Shcherbakov (2004) recently observed a systematic increase of overall intensity of $[\text{pTRM}\uparrow^0] + [t\uparrow^0]$, although a different initial state was used (see Table 3 for comparison).

For coarse-grained magnetites (e.g., Fig. 6b), we confirm that the magnetizations are continuously driven to more stable states during repeated heat treatments, following the Markov process (Fabian, 2003). Instability of magnetization in MD grains introduces a few interesting features in Thellier experiments. First, a progressive increase of pTRM provides another source that can amplify the non-linear features in the Arai plots. Of course, the violation of reciprocity is the major contributor for non-linear behavior. For the Coe method, it is possible that multiple heatings for in-field steps can slightly shift each given data-point toward the right in Arai plots (caused by the progressive increase of pTRM acquisition), toward the ideal line. By analogy, we would expect the same to be true for the Aitken method. Second, a systematic decrease of pTRM tail checks during multiple heatings may limit the use of the pTRM tail check as a sample selection criterion.

Do we need to examine the stability of pTRMs and pTRM tail checks in practice? For samples that contain coarse-grained magnetites, the pTRMs and pTRM tail checks are definitely not stable, but migrate towards more stable remanence states during multi-cycle heat treatments (Figs. 6b and 7b). However, we believe that the practical impact of the instability of magnetization in coarse-grained magnetite is likely to be minimal because reliable paleointensities are rarely (if ever) determined using coarse-grained magnetites. In fine-grained magnetites, however, both pTRMs and pTRM tail checks are stable and reproducible (Figs. 2–5, 6a, and 7a).

6. Conclusion

- (1) The magnitude of pTRM is always larger when the pTRMs were induced from a thermally demagnetized state than those produced in samples with a pre-existing TRM when the field used to impart pTRM is equal in magnitude and parallel to that used to produce TRM.
- (2) The pTRMs progressively increased during multi-cycle heat-treatments, while pTRM tail checks progressively decreased.

- (3) For coarse-grained magnetites, both (1) and (2) enhance the non-linear features of the Arai plot. However, their practical impact would be minimal because reliable paleointensities are difficult to obtain from multi-domain magnetites.

Acknowledgments

This research was supported by NSF grant EAR0229498 to L. Tauxe. Peter Riisager provided helpful discussions. We thank Jason Steindorf for help with the measurements.

References

- Aitken, M.J., Allsop, A.L., Bussell, G.D., Winter, M.B., 1988. Determination of the intensity of the Earth's magnetic field during archeological times: reliability of the Thellier technique. *Rev. Geophys.* 26, 3–12.
- Ambatiello, A., Fabian, K., Hoffmann, V., 1999. Magnetic domain structure of multidomain magnetite as a function of temperature: Observation by Kerr microscopy. *Phys. Earth Planet. Int.* 112, 55–80.
- Biggin, A.J., Bohnel, H.N., 2003. A method to reduce the curvature of Arai plots produced during Thellier paleointensity experiments performed on multidomain grains. *Geophys. J. Int.* 155, F13–F19.
- Bol'shakov, A.S., Shcherbakova, V.V., 1979. A thermomagnetic criterion for determining the domain structure of ferrimagnetics. *Izv. Acad. Sci. U.S.S.R. Phys. Solid Earth Engl. Trans.* 15, 111–117.
- Carlut, J., Kent, D.V., 2002. Grain size dependent paleointensity results from very recent mid-oceanic ridge basalts. *J. Geophys. Res.* 107 (B3), 2049, doi:10.1029/2001JB000439.
- Calvallo, C., Camps, P., Ruffet, G., Henry, B., Poidras, T., 2003. Mono Lake or Laschamp geomagnetic event recorded from lava flows in Amsterdam Island (southeastern Indian Ocean). *Geophys. J. Int.* 154, 762–782.
- Coe, R.S., 1967. Paleointensities of the Earth's magnetic field determined from tertiary and quaternary rocks. *J. Geophys. Res.* 72, 3247–3262.
- Day, R., Fuller, M., Schmidt, V.A., 1977. Hysteresis properties of titanomagnetites: Grain size and composition dependence. *Phys. Earth Planet. Int.* 13, 260–267.
- Dunlop, D.J., Özdemir, Ö., 2000. Effect of grain size and domain state on thermal demagnetization tails. *Geophys. Res. Lett.* 27, 1311–1314.
- Dunlop, D.J., Özdemir, Ö., 2001. Beyond Néel's theories: Thermal demagnetization of narrow-band partial thermoremanent magnetization. *Phys. Earth Planet. Int.* 126, 43–57.
- Enkin, R.J., Dunlop, D.J., 1987. A micromagnetic study of pseudo-single-domain remanence in magnetite. *J. Geophys. Res.* 92, 12,726–12,740.
- Enkin, R.J., Williams, W., 1994. Three-dimensional micromagnetic analysis of stability in fine magnetic grains. *J. Geophys. Res.* 99, 611–618.
- Fabian, K., 2000. Acquisition of thermoremanent magnetization in weak magnetic field. *Geophys. J. Int.* 142, 478–486.
- Fabian, K., 2001. A theoretical treatment of paleointensity determination experiments on rocks containing pseudo-single or multi domain magnetic particles. *Earth Planet. Sci. Lett.* 188, 45–58.

- Fabian, K., 2003. Statistical theory of weak field thermoremanent magnetization in multidomain particle ensembles. *Geophys. J. Int.* 155, 479–488.
- Fabian, K., Shcherbakov, V.P., 2004. Domain state stabilization by iterated thermal magnetization processes. *Geophys. J. Int.* 159, 486–494.
- Halgedahl, S.L., 1991. Magnetic domain patterns observed on synthetic Ti-rich titanomagnetite as a function of temperature and in states of thermoremanent magnetization. *J. Geophys. Res.* 96, 3943–3972.
- Halgedahl, S.L., 1993. Experiments to investigate the origin of anomalously elevated unblocking temperatures. *J. Geophys. Res.* 98, 22,443–22,460.
- Heider, F., 1990. Temperature dependence of domain structure in natural magnetite and its significance for multidomain TRM models. *Phys. Earth Planet. Int.* 65, 54–61.
- Heider, F., Halgedahl, S.L., Dunlop, D.J., 1988. Temperature dependence of magnetic domains in magnetite crystals. *Geophys. Res. Lett.* 15, 499–502.
- Krasa, D., Heunemann, C., Leonhardt, R., Petersen, N., 2003. Experimental procedure to detect multidomain remanence during Thellier–Thellier experiments. *Phys. Chem. Earth* 28, 681–687.
- Leonhardt, R., Krasa, D., Coe, R.S., 2004. Multidomain behavior during Thellier paleointensity experiments: A phenomenological model. *Phys. Earth Planet. Int.* 147, 127–140.
- Liu, Q., Yu, Y., 2004. Multi-cycle low-temperature demagnetization (LTD) of multi-domain magnetite. *J. Mag. Mag. Mater.* 283, 150–156.
- Néel, L., 1955. Some theoretical aspects of Rock-Magnetism. *Adv. Phys.* 4, 191–243.
- Riisager, J., Perrin, M., Riisager, P., Ruffet, G., 2000. Paleomagnetism, paleointensity, and geochronology of Miocene basalts and baked sediments from Velay Orinetal, French Massif Central. *J. Geophys. Res.* 105, 883–896.
- Riisager, P., Riisager, J., 2001. Detecting multidomain magnetic grains in Thellier paleointensity experiments. *Phys. Earth Planet. Int.* 125, 11–117.
- Shcherbakov, V.P., Shcherbakova, V., 2001. On the stability of Thellier method of paleointensity determination on pseudo-single-domain and multidomain grains. *Geophys. J. Int.* 146, 20–30.
- Shcherbakov, V.P., Shcherbakova, V., Vinogradov, Y.K., Heider, F., 2001. Thermal stability of pTRM created from different magnetic states. *Phys. Earth Planet. Int.* 126, 59–73.
- Shcherbakova, V., Shcherbakov, V.P., Heider, F., 2000. Properties of partial thermoremanent magnetization in PSD and MD magnetite grains. *J. Geophys. Res.* 105, 767–782.
- Tauxe, L., Staudigel, H., 2004. Strength of the geomagnetic field in the Cretaceous Normal Superchron: New data from submarine basaltic glass of the Troodos Ophiolite. *Geochem. Geophys. Geosyst.* 5 (2), doi:10.1029/2003GC000635, Q02H06.
- Thellier, E., Thellier, O., 1959. Sur l'intensité du champ magnétique terrestre dans le passé historique et géologique. *Ann. Geophys.* 15, 285–378.
- Vinogradov, Y.K., Markov, G.P., 1989. On the effect of low temperature heating on the magnetic state of multidomain magnetite. In: *Investigations in Rock Magnetism and Paleomagnetism*. Institute of the Physics of the Earth, Moscow, pp. 31–39 (in Russian).
- Winklehofer, M., Fabian, K., Heider, F., 1997. Magnetic blocking temperature of magnetite calculated with a three-dimensional micro-magnetic model. *J. Geophys. Res.* 102, 22,695–22,709.
- Worm, H.U., Jackson, M., Kelso, P., Banerjee, S.K., 1988. Thermal demagnetization of partial thermoremanent magnetization. *J. Geophys. Res.* 93, 12,196–12,204.
- Yu, Y., 1998. Rock magnetic and paleomagnetic experiments on hemoilmenites and titanomagnetites in some volcanic rocks from Japan, M.Sc. thesis.
- Yu, Y., Dunlop, D.J., 2001. Paleointensity determination on the late Precambrian Tudor Gabbro, Ontario. *J. Geophys. Res.* 106, 26,331–26,344.
- Yu, Y., Dunlop, D.J., 2002. Multivectorial paleointensity determination from the Cordova Gabbro, southern Ontario. *Earth Planet. Sci. Lett.* 203, 983–998.
- Yu, Y., Dunlop, D.J., 2003. On partial thermoremanent magnetization tail checks in Thellier paleointensity determination. *J. Geophys. Res.* 108 (B11), 2523, doi:10.1029/2003JB002420.
- Yu, Y., Tauxe, L., Genevey, A., 2004. Towards an optimal geomagnetic field intensity determination technique. *Geochem. Geophys. Geosyst.* 5 (2), doi:10.1029/2003GC000630, Q02H07.
- Yu, Y., Tauxe, L., 2005. Testing the IZZI protocol of geomagnetic field intensity determination. *Geochem. Geophys. Geosyst.* 6 (5), doi:10.1029/2004GC000840, Q05H17.